One-Pot Synthesis of Symmetric Octithiophenes from Asymmetric β-Alkylsulfanyl Bithiophenes

Adele Mucci,* Francesca Parenti, Rita Cagnoli, Rois Benassi, Alessio Passalacqua, Lisa Preti, and Luisa Schenetti

Dipartimento di Chimica, Università degli Studi di Modena e Reggio Emilia, via G. Campi 183, 41100 Modena, Italy

Received June 23, 2006; Revised Manuscript Received September 5, 2006

ABSTRACT: Starting from 4-(octylsulfanyl)-2,2′-bithiophene, 4-bromo-4′-(octylsulfanyl)-2,2′-bithiophene, 4-iodo-4′-(octylsulfanyl)-2,2′-bithiophene, 4-bromo-4′-[(*S*)-2-methylbutylsulfanyl]-2,2′-bithiophene, and 4-iodo-4′-[(*S*)-2-methylbutylsulfanyl]-2,2′-bithiophene, a new series of symmetrically β-substituted octithiophenes were synthesized by one-pot oxidative coupling with $FeCl_3$. The octithiophenes obtained are soluble in common organic solvents and show different solvatochromic properties depending on the substitution type. In particular, the bromine atom exerts a positive influence on the supramolecular organization: the brominated octithiophenes display high filmability, solvatochromism, and CD induced by aggregation (when the chiral 2-methylbutylsulfanyl group is present), properties usually observed for polythiophenes. Density functional theory (DFT) calculations were carried out an a model bithiophene (4-substituted with a methylsulfanyl group) in order to understand the possible mechanism of the growth, the regiochemistry, and the reason for the polymerization leads to an octithiophene.

Introduction

Structurally well-defined oligothiophenes (OTs) have been extensively investigated as model compounds to better understand the properties of the related α-conjugated semiconducting polymers. More recently, they have attracted increasing attention as a low-cost alternative to silicon materials for electronic device applications, such as field effect transistors (FET),[1−3] organic light-emitting diodes (OLED),[4,5] photovoltaic cells,[6,7] and sensors.[8,9] The good performances of α-conjugated oligomers are strongly related to the fact that they are materials with a rigorously defined chain and conjugation length, permitting a better control on the supramolecular organization and thus well-defined optical properties in the devices.[10−12] Because, in most applications, conjugated oligomers are used in the solid state, the fact of being monodisperse materials, which often can be crystallized and in many cases also sublimed, permits the investigation of their solid-state properties in crystals or in vapor-deposited thin films.[13] On the other hand, the solubility of these materials in organic solvents or water is a prerequisite for the formation of films by spin-coating or casting techniques, and in this respect, it is worthwhile stressing that oligomers are more soluble than related polymers, and an improved solubility, together with the possibility of a modulation of the chemical−physical properties, can be achieved by adequate substitutions in the β-position of the thiophene ring.

Our previous studies on alkylsulfanyl bithiophenes have shown that oxidative polymerization with $FeCl_3$ of 4,4′-bis-(alkylsulfanyl)-2,2′-bithiophenes afforded high-molecular-weight polymers with very interesting chemical physical properties, such as a small band gap between ground and excited states that allows for easy p- and n-electrochemical doping (thanks to the electrodonating sulfur atom), a marked solvatochromism, a high solubility in organic solvents, and a good filmability.[14,15] The same reaction performed on 3,3′-bis(butylsulfanyl)-2,2′-bithiophene[16] and on 3-(butylsulfanyl)-2,2′-bithiophene[17] afforded two hexamers in high yields.

* Corresponding author. E-mail: mucci.adele@unimo.it.

Scheme 1

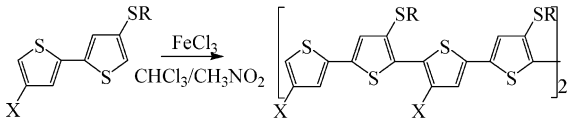

1	X=H, R= $(CH_2)_7CH_3$	**OT1**
2	X= Br, R=$(CH_2)_7CH_3$	**OT2**
3	X= I, R=$(CH_2)_7CH_3$	**OT3**
4	X= Br, R=$CH_2CH(CH_3)CH_2CH_3$	**OT4**
5	X= I, R= $CH_2C\ H(CH_3)CH_2CH_3$	**OT5**

We pursued these investigations with the aim of gaining a further insight into the reactivity of β-alkylsulfanyl-substituted bithiophenes, and in this paper, we report on the synthesis and oxidative polymerization of bithiophenes **1**−**5** (Scheme 1)**.** Bithiophene **1** is formed by an octylsulfanyl β-substituted and an unsubstituted thiophene ring, while bithiophenes **2**−**5** are formed by two β-substituted thiophene rings, bearing a halogen atom and an alkylsulfanyl group, with tail-to-tail (TT) regiochemistry.

Astonishingly, five symmetric octithiophenes **OT1**−**OT5** with the same regiochemistry were obtained in high percentage from bithiophenes **1**−**5** through oxidative polymerization with $FeCl_3$. All synthesized oligomers are soluble in common organic solvents ($CHCl_3$, THF, DMF, DMSO) and thus easily processable and characterizable. The two bromo-functionalized octithiophenes form free-standing films and show a remarkable solvatochromism, properties very similar to those observed for alkylsulfanyl polythiophenes.[14,15]

A computational study carried out at the DFT level on 4-(methylsulfanyl)-2,2′-bithiophene, aimed at establishing the possible sequences of the coupling reactions leading to the formation of an octithiophene with the experimental regiochemistry, suggests a head-to-tail (HT)/head-to-head (HH) two-step mechanism.

Experimental Section

General Techniques. All air- or moisture-sensitive reactions were performed under prepurified nitrogen or argon with dry

10.1021/ma0614141 CCC: $33.50
Published on Web 10/26/2006

glassware. Tetrahydrofuran (THF) and diethyl ether were distilled from sodium and benzophenone prior to use. Pyridine, toluene, chloroform, and nitromethane were dried by standard procedures. Anhydrous iron(III) chloride was purchased from Fluka.

^{1}H and ^{13}C NMR spectra were recorded with Bruker Avance400 spectrometer operating at 400.13 and 100.61 MHz, respectively, and with a Bruker DPX-200 spectrometer operating at 200.13 MHz. UV−Vis spectra were recorded using a Perkin-Elmer Lambda Bio 20 UV−visible spectrophotometer. CD spectra were recorded with a JASCO J-710 spectropolarimeter. Mass spectra were recorded using a Finnigan MAT SSQ 710 A mass spectrometer equipped with a direct inlet probe (DIP). IR spectra were recorded using a Perkin-Elmer I-series FT-IR microscope equipped with a diamond cell.

Synthesis of 5-Bromo-3-(octylsulfanyl)-2-(trimethylsilyl)thiophene.[18] (a) To a solution of 3-methoxythiophene (2.00 g, 17.4 mmol) in toluene (20 mL), toluene-4-sulfonic acid (0.14 g, 0.8 mmol) and octanthiol (2.56 g, 17.4 mmol) were added. The reaction mixture was stirred for 20 h at 80 °C, then it was allowed to cool to room temperature and diluted with diethyl ether. The organic layer was washed with water dried over $MgSO_4$, filtered, and vacuum evaporated, obtaining 3.72 g (93%) of 3-(octylsulfanyl)-thiophene, as a pale-yellow oil; bp 111 °C/0.5 mmHg. ^{1}H NMR (200 MHz, $CDCl_3$, TMS δ): 7.33 (dd, J = 5.0, 3.0 Hz, 1H, H-5), 7.13 (dd, J = 1.3, 3.0 Hz, 1H, H-2), 7.04 (dd, J = 1.3, 5.0 Hz, 1H, H-4), 2.86 (t, J = 7.2 Hz, 2H, α-CH_2), 1.64 (m, 2H, β-CH_2), 1.41 (m, 2H, γ-CH_2), 1.29 (m, 8H, 4 CH_2), 0.90 (t, J = 6.9 Hz, 3H, CH_3). (b) To a solution of 3-(octylsulfanyl)thiophene (2.64 g, 11.6 mmol) in glacial acetic acid (8 mL), *N*-bromosuccinimide (2.06 g, 11.6 mmol) was added in small portions, maintaining the temperature between 15 and 17 °C. After stirring for 2 h at 25 °C, the mixture was poured in iced water and extracted with diethyl ether. The organic layers were washed with a saturated solution of $NaHCO_3$ with water and dried over $MgSO_4$. After removal of the solvent, the residue was distilled under reduced pressure to give 3.45 g (97%) of 2-bromo-3-(octylsulfanyl)thiophene as brown oil; bp 142−145 °C/0.3 mmHg). ^{1}H NMR (400 MHz, $CDCl_3$, TMS δ): 7.27 (d, J = 5.4 Hz, 1H, H-5), 6.94 (d, J = 5.4 Hz, 1H, H-4), 2.86 (t, J = 7.2 Hz, 2H, α-CH_2), 1.60 (m, 2H, β-CH_2), 1.41 (m, 2H, γ-CH_2), 1.29 (m, 8H, 4 CH_2), 0.89 (t, J = 6.9 Hz, 3H, CH_3). (c) To a cooled solution (−70 °C) of butyllithium in *n*-hexane (1.6 M, 3.5 mL, 5.6 mmol), a solution of diisopropylamine (0.61 g, 6 mmol) in dry THF (6 mL) was added. The temperature was kept at −30 °C for 1 h and then lowered to −80 °C. A solution of 2-bromo-3-(octylsulfanyl)thiophene (1.43 g, 4.6 mmol) in dry THF (8 mL) was quickly added, and stirring was continued for 30 min at the same temperature. A solution of chlorotrimethylsilane (0.51 g, 4.6 mmol) in dry THF (4 mL) was slowly added, and the stirring was continued for 30 min at −80 °C. The mixture was then poured in 1 M HCl extracted with diethyl ether, washed with water, and then dried ($MgSO_4$). After removal of the solvent, the residue was purified by column chromatography on silica gel (petroleum ether bp 40−60 °C) giving 1.19 g (67%) of 5-bromo-3-(octylsulfanyl)-2-(trimethylsilyl)thiophene as pale-yellow oil; ^{1}H NMR (400 MHz, $CDCl_3$, TMS δ): 7.09 (s, 1H, H-4), 2.80 (t, J = 7.2 Hz, 2H, α-CH_2), 1.62 (m, 2H, β-CH_2), 1.39 (m, 2H, γ-CH_2), 1.29 (m, 8H, 4 CH_2), 0.90 (t, J = 6.9 Hz, 3H, CH_3), 0.38 (s, $J_{CH3,Si}$ = 6.9 Hz, 9H, Si-$(CH_3)_3$). Elemental analysis $C_{15}H_{27}BrS_2Si$ Calcd: C, 47.47; H, 7.17; S, 16.90. Found: C, 47.52; H, 7.20; S, 16.41.

Synthesis of (+)-5-Bromo-3-[(*S*)-2-methylbutylsulfanyl]-2-(trimethylsilyl)thiophene. (a) A solution of potassium *tert*-butylate (37.25 g, 0.33 mol) in dry ethanol (110 mL) was cooled to 0 °C, then a solution of 3-mercaptothiophene[19] (27.00 g, 0.23 mol) in dry ethanol (5 mL) was slowly added, keeping the temperature below 10 °C. A solution of 1-bromo-2-methylbutane $[\alpha]_D^{20}$ = +4 (c = 1.1, $CHCl_3$) (35.15 g, 0.23 mol) in dry ethanol (20 mL) was dropped, maintaining the temperature between 0 and 10 °C. The reaction mixture was refluxed for 1 h and 30 min, cooled, and then poured in an ice−water bath and extracted with diethyl ether. The organic layer was washed with water and dried over $MgSO_4$, filtered, and fractionally distilled to give 12.71 g (68%) of (+)-3-[(*S*)-2-methylbutylsulfanyl]thiophene; bp 87 °C at 2 mmHg; $[\alpha]_D^{20}$ = +26 (c = 1.0, $CHCl_3$). ^{1}H NMR (400 MHz, $CDCl_3$, TMS δ): 7.31 (dd, J = 5.0, 3.0 Hz, 1H, H-5), 7.09 (dd, J = 3.0, 1.3 Hz, 1H, H-2), 7.02 (dd, J = 5.0, 1.3 Hz, 1H, H-4), 2.88 (dd, J = 12.5, 5.8 Hz, 1H, H-α), 2.69 (dd, J = 12.5, 7.5 Hz, 1H, H-α′), 1.63 (m, 1H, H-β), 1.52 (m, 1H, H-γ), 1.25 (m, 1H, H-γ′), 1.01 (d, J = 6.5 Hz, 3H, γ-CH_3), 0.89 (t, J = 7.4 Hz, 3H, δ-CH_3). (b) As above, starting from (+)-3-[(*S*)-2-methylbutylsulfanyl]thiophene (10.2 g, 54 mmol), 11.2 g (77%) of 2-bromo-3-[(*S*)-2-methylbutylsulfanyl]-thiophene were obtained as a brown oil; bp 77 °C/0.01 mmHg. ^{1}H NMR (200 MHz, $CDCl_3$, TMS δ): 7.25 (d, J = 5.7 Hz, 1H, H-5), 6.92 (d, J = 5.7 Hz, 1H, H-4), 2.87 (dd, J = 12.5, 5.6 Hz, 1H, H-α), 2.68 (dd, J = 12.5, 7.3 Hz, 1H, H-α′), 1.53 (m, 2H, H-β and H-γ), 1.25 (m, 1H, H-γ′), 1.01 (d, J = 6.6 Hz, 3H, γ-CH_3), 0.89 (t, J = 7.4 Hz, 3H, δ-CH_3). (c) As above, starting from 2-bromo-3-[(*S*)-2-methylbutylsulfanyl]thiophene (7.07 g, 26.6 mmol), 3.61 g (52%) of pale-yellow oil were obtained; $[\alpha]_D^{20}$ = +26 (c = 1.0, $CHCl_3$). ^{1}H NMR (400 MHz, $CDCl_3$, TMS δ): 7.07 (s, 1H, H-4), 2.82 (dd, J = 12.4, 5.7 Hz, 1H, H-α), 2.65 (dd, J = 12.4, 7.4 Hz, 1H, H-α′), 1.53 (m, 2H, H-β and H-γ), 1.25 (m, 1H, H-γ′), 0.99 (d, J = 6.6 Hz, 3H, γ-CH_3), 0.89 (t, J = 7.4 Hz, 3H, δ-CH_3), 0.42 (s, $J_{CH3,Si}$ = 6.9 Hz, 9H, 5-$SiMe_3$). Elemental analysis $C_{12}H_{21}BrS_2Si$ Calcd: C, 42.72; H, 6.27; S, 19.01. Found: C, 42.54; H, 6.35; S, 18.89.

Synthesis of 2-(Trimethylsilyl)-5-(trimethylstannyl)thiophene. A solution of 5-bromo-2-(trimethylsilyl)thiophene[20] (4.20 g, 16.5 mmol) in THF (60 mL) was cooled to −80 °C; butyllithium in *n*-hexane (1.6 M, 10.3 mL, 16.5 mmol) was slowly added, keeping the temperature below −70 °C. The mixture was stirred at −80 °C for 30 min, then a solution of trimethyltin chloride in THF (1 M, 16.5 mL, 16.5 mmol) was dropwise added, and the stirring was continued for 30 min at −80 °C. The mixture was warmed to room temperature, poured in iced water, and then extracted with diethyl ether. After removal of the solvent and vacuum distillation, a white solid 1.70 g (30%) was obtained; bp 66 °C/0.1 mmHg. ^{1}H NMR (400 MHz, $CDCl_3$, TMS δ): 7.40 (d, J = 3.1 Hz, $J_{H-3,Sn}$ = 3.8 Hz, 1H, H-3), 7.30 (d, J = 3.1 Hz, $J_{H-4,Sn}$ = 24.0 Hz, 1H, H-4), 0.37 (s, $J_{CH3,\ ^{119}Sn}$ = 57.7 Hz, $J_{CH3,\ ^{117}Sn}$ = 55.1 Hz, 9H, 5-$SnMe_3$), 0.33 (s, $J_{CH3,Si}$ = 6.6 Hz, 9H, 2-$SiMe_3$). Elemental analysis $C_{10}H_{20}SSiSn$ Calcd: C, 37.64; H, 6.32; S, 10.05. Found: C, 37.49; H, 6.44; S, 9.85.

Synthesis of 3-Bromo-2-(trimethylsilyl)-5-(trimethylstannyl)-thiophene. (a) According to ref 21, to a solution of butyllithium in *n*-hexane (1.6 M, 27.5 mL, 44 mmol) in dry THF (20 mL) at −70 °C, a solution of diisopropylamine (4.82 g, 48 mmol) in dry THF (7 mL) was added. The temperature was raised to −30 °C, and stirring was continued at this temperature for 1 h. To the reaction mixture cooled to −80 °C, a solution of 2,3-dibromothiophene (8.90 g, 37 mmol) in dry THF (7 mL) was quickly added, and the stirring was continued for 30 min at the same temperature. The intermediate thus formed was trapped by slow addition of a solution of chlorotrimethylsilane (4.01 g, 37 mmol) in dry THF (4 mL), and stirring was continued for 30 min at −80 °C. The mixture was then poured into 1 M HCl extracted with diethyl ether. The organic layers were washed with water and dried over $MgSO_4$. The solvent was removed, and the residue was distilled under reduced pressure to give 10.41 g (90%) of 3,5-dibromo-2-(trimethylsilyl)-thiophene as a pale- yellow oil; bp 95−97 °C/2 mmHg. ^{1}H NMR (200 MHz, $CDCl_3$, TMS) δ): 7.02 (s, 1H, H-4), 0.38 (s, $J_{CH3,Si}$ = 6.9 Hz, 9H, $SiMe_3$). (b) According to ref 22, to a solution of 3,5-dibromo-2-(trimethylsilyl)thiophene (3.02 g, 7.5 mmol) in dry THF (40 mL) at −80 °C, a solution of butyllithium in *n*-hexane (1.6 M, 6 mL, 9.6 mmol) was dropwise added under stirring, and stirring was continued at this temperature for 40 min. A solution of trimethyltin chloride in dry THF (1 M, 10.5 mL, 10.5 mmol) was then dropwise added, and the reaction mixture was allowed to reach room temperature, poured in an ice−water bath, and extracted with diethyl ether. The organic layers were washed with water, dried over $MgSO_4$, the solvent evaporated, and the crude product was fractionally distilled obtaining 1.84 g (48%) of a pale-yellow oil; bp 93−95 °C/0.2 mmHg. ^{1}H NMR (200 MHz, $CDCl_3$, TMS) δ):

7.15 (s, 1H, H-4), 0.39 (s, $J_{CH3,Si}$ = 6.9 Hz, 9H, $SiMe_3$), 0.37 (s, $J_{CH3,}{}^{119}{}_{Sn}$ = 57.7 Hz, $J_{CH3,}{}^{117}{}_{Sn}$ = 55.3 Hz, 9H, $SnMe_3$). Elemental analysis $C_{10}H_{19}BrSSiSn$ Calcd: C, 30.18; H, 4.81; S, 8.06. Found: C, 30.25; H, 4.71; S, 7.92.

Synthesis of 4-(Octylsulfanyl)-2,2′-bithiophene (1). (a) A solution of 5-bromo-3-(octylsulfanyl)-2-(trimethylsilyl)thiophene (1.37 g, 3.6 mmol) in dry toluene (14 mL) was dropwise added to a stirred solution of 2-(trimethylsilyl)-5-(trimethylstannyl)thiophene (1.15 g, 3.6 mmol) and tetrakis(triphenylphosphine)palladium(0) (0.33 g, 0.29 mmol) in dry toluene (8 mL) at 105 °C. The reaction mixture was stirred for 3 days at this temperature. After cooling, it was transferred into a separatory funnel, diluted with diethyl ether, and washed with saturated $NaHCO_3$ and water. The organic phase was dried over $MgSO_4$ and evaporated, obtaining 1.54 g of 4-(octylsulfanyl)-5,5′-bis(trimethylsilyl)-2,2′-bithiophene that was directly used without further purification in the subsequent desilylation step. (b) In analogy to ref 20, to a solution of 4-(octylsulfanyl)-5,5′-bis(trimethylsilyl)-2,2′-bithiophene (1.54 g, 3.4 mmol) in benzene (4 mL), hydriodic acid (13.6 mmol, 1.7 mL, 57%) was dropwise added. The mixture was stirred at room temperature for 2 h before being poured into water. The aqueous phase was extracted with diethyl ether, and the organic extracts were washed with 1 M NaOH and brine and dried over $MgSO_4$. The solvent was removed by reduced pressure to provide a brown oil that was purified by column chromatography on silica gel (petroleum ether bp 40−60 °C), giving 0.42 g (40%) of **1** as a white solid after removal of the residual eluant; mp 26−27 °C. ^{1}H NMR (400 MHz, $CDCl_3$, TMS δ): 7.23 (dd, J = 5.0, 1.2 Hz, 1H, H-5′), 7.16 (dd, J = 3.6, 1.2 Hz, 1H, H-3′), 7.07 (d, J = 1.4 Hz, 1H, H-3), 7.01 (dd, J = 5.0, 3.6 Hz, 1H, H-4′), 6.97 (d, J = 1.4 Hz, 1H, H-5), 2.86 (t, J = 7.2 Hz, 2H, α-CH_2), 1.65 (m, 2H, β-CH_2), 1.41 (m, 2H, γ-CH_2), 1.28 (m, 8H, 4 CH_2), 0.88 (t, J = 6.9 Hz, 3H, CH_3). ^{13}C NMR (100.61 MHz, $CDCl_3$, TMS δ): 137.9 (C-2), 136.8 (C-2′), 133.1 (C-4), 127.8 (C-4′), 125.9 (C-3), 124.7 (C-5′), 123.9 (C-3′), 121.6 (C-5), 35.1 (C-α), 31.7 (C-ζ), 29.3 (C-β), 29.1 (C-δ, C-ϵ), 28.6 (C-γ), 22.6 (C-η), 14.0 (C-θ). Elemental analysis $C_{16}H_{22}S_3$ Calcd: C, 61.88; H, 7.14; S, 30.98. Found: C, 61.74; H, 7.13; S, 30.66.

Synthesis of 4-Bromo-4′-(octylsulfanyl)-2,2′-bithiophene (2). (a) From 1.25 g (3.1 mmol) of 5-bromo-3-(octylsulfanyl)-2-(trimethylsilyl)thiophene and 1.19 g (3.1 mmol) of 3-bromo-2-(trimethylsilyl)-5-(trimethylstannyl)thiophene, 1.34 g of 4-bromo-4′-(octylsulfanyl)-5,5′-bis(trimethylsilyl)-2,2′-bithiophene (brown oil) were obtained. (b) From 1.34 g (2.5 mmol) of 4-bromo-4′-(octylsulfanyl)-5,5′-bis(trimethylsilyl)-2,2′-bithiophene in benzene (50 mL) and 0.9 mL (5.1 mmol) of hydriodic acid (48%), in 16 h, 0.34 g (35%) of **2** as a pale-yellow solid were obtained; mp 36 °C.; ^{1}H NMR (400 MHz, $CDCl_3$, TMS δ): 7.12 (d, J = 1.4 Hz, 1H, H-5), 7.07_2 (d, J = 1.4 Hz, 1H, H-3′), 7.06_8 (1H, d, J = 1.4 Hz, H-3), 7.01 (d, J = 1.4 Hz, 1H, H-5′), 2.86 (t, J = 7.2 Hz, 2H, α-CH_2), 1.65 (m, 2H, β-CH_2), 1.41 (m, 2H, γ-CH_2), 1.27 (m, 8H, 4 CH_2), 0.88 (t, J = 6.9 Hz, 3H, CH_3). ^{13}C NMR (100.61 MHz, $CDCl_3$, TMS δ): 138.0 (C-2), 136.4 (C-2′), 133.5 (C-4′), 126.5 (C-3′), 126.3 (C-3), 122.3 (C-5′), 121.7 (C-5), 110.4 (C-4), 35.2 (C-α), 31.8 (C-ζ), 29.3 (C-β), 29.1 (C-δ, C-ϵ), 28.7 (C-γ), 22.6 (C-η), 14.1 (C-θ). Elemental analysis $C_{16}H_{21}BrS_3$ Calcd: C, 49.35; H, 5.44; S, 24.70. Found: C, 49.45; H, 5.37; S, 24.32.

Synthesis of 4-Iodo-4′-(octylsulfanyl)-2,2′-bithiophene (3). As described in the above procedure (b), from 2.01 g (3.8 mmol) of 4-bromo-4′-(octylsulfanyl)-5,5′-bis(trimethylsilyl)-2,2′-bithiophene in benzene (95 mL) and 2.0 mL (15.4 mmol) of hydriodic acid (57%), in 64 h, 0.72 g (42%) of **3** as a pale-yellow viscous oil were obtained. ^{1}H NMR (400 MHz, $CDCl_3$, TMS δ): 7.28 (d, J = 1.4 Hz, 1H, H-5), 7.12 (d, J = 1.4 Hz, 1H, H-3), 7.07 (1H, d, J = 1.4 Hz, 1H, H-3′), 7.01 (d, J = 1.4 Hz, 1H, H-5′), 2.86 (t, J = 7.2 Hz, 2H, α-CH_2), 1.65 (m, 2H, β-CH_2), 1.41 (m, 2H, γ-CH_2), 1.27 (m, 8H, 4 CH_2), 0.88 (t, J = 6.9 Hz, 3H, CH_3). ^{13}C NMR (100.61 MHz, $CDCl_3$, TMS δ): 138.8 (C-2), 136.1 (C-2′), 133.6 (C-4′), 131.0 (C-3), 127.7 (C-5), 126.6 (C-3′), 122.4 (C-5′), 77.6 (C-4), 35.2 (C-α), 31.8 (Cζ), 29.6 (C-β), 29.2 (C-δ), 29.1 (C-ϵ), 28.7 (C-γ), 22.7 (C-η), 14.1 (C-θ). Elemental analysis $C_{16}H_{21}IS_3$ Calcd: C, 44.03; H, 4.85; S, 22.04. Found: C, 43.89; H, 4.91; S, 21.93.

Synthesis of 4-Bromo-4′-[(*S*)-2-methylbutylsulfanyl]-2,2′-bithiophene (4). (a) From 1.07 g (3.2 mmol) of 5-bromo-3-[(*S*)-2-methylbutylsulfanyl]-2-(trimethylsilyl)thiophene and 1.26 g (3.2 mmol) of 3-bromo-2-(trimethylsilyl)-5-(trimethylstannyl)thiophene, 1.35 g of 4-bromo-4′-[(*S*)-2-methylbutylsulfanyl]-5,5′-bis(trimethylsilyl)-2,2′-bithiophene as crude product (brown oil) were obtained. (b) A solution of crude substrate (1.35 g, 2.7 mmol) in THF (60 mL) and water (1.7 mL) was cooled to −5 °C. A solution of tetrabutylammonium fluoride (1 M in THF, 14.2 mL, 14.2 mmol) was slowly added to the reaction mixture. After stirring for 4 h at −5 °C, sodium bicarbonate (5% aq, 50 mL) was added, then the mixture was extracted with diethyl ether and washed with water. The organic layers were dried over $MgSO_4$ then filtered and evaporated, and the crude product was purified by column chromatography on silica gel (petroleum ether bp 40−60 °C), giving 0.34 g (36%) of **4** a pale-yellow viscous oil. ^{1}H NMR (400 MHz, $CDCl_3$, TMS δ): 7.12 (d, J = 1.5 Hz, 1H, H-5), 7.07 (d, J = 1.4 Hz, 1H, H-3′), 7.06 (d, J = 1.5 Hz, 1H, H-3), 6.98 (d, J = 1.4 Hz, 1H, H-5′), 2.89 (dd, J = 12.5, 5.9 Hz, 1H, H-α), 2.70 (dd, J = 12.5, 7.5 Hz, 1H, H-α′), 1.65 (m, 1H, H-β), 1.55 (m, 1H, H-γ), 1.25 (m, 1H, H-γ′), 1.03 (d, J = 6.6 Hz, 3H, γ-CH_3), 0.89 (t, J = 7.4 Hz, 3H, δ-CH_3). ^{13}C NMR (100.61 MHz, $CDCl_3$, TMS δ): 138.0 (C-2), 136.4 (C-2′), 134.1 (C-4′), 126.4 (C-3′), 126.3 (C-3), 121.8 (C-5′), 121.7 (C-5), 110.3 (C-4), 42.2 (C-α), 34.6 (C-β), 28.6 (C-γ), 18.8 (C-γ′), 11.2 (C-δ). Elemental analysis $C_{13}H_{15}BrS_3$ Calcd: C, 44.95; H, 4.35; S, 27.69. Found: C, 45.01; H, 4.32; S, 27.45.

Synthesis of 4-Iodo-4′-[(*S*)-2-methylbutylsulfanyl]-2,2′-bithiophene (5). As described for **3**, from 4-bromo-4′-[(*S*)-2-methylbutylsulfanyl]-5,5′-bis(trimethylsilyl)-2,2′-bithiophene 2.59 g (5.4 mmol) in benzene (80 mL) and 2.9 mL (22.0 mmol) of hydriodic acid (57%), in 64 h, 1.17 g (55%) of **5**, as a pale-yellow solid, were obtained; mp 34 °C; $[\alpha]^{20}{}_D$ = +13.7 (c = 1.0 in $CHCl_3$). ^{1}H NMR (400 MHz, $CDCl_3$, TMS δ): 7.28 (d, J = 1.4 Hz, 1H, H-5), 7.13 (d, J = 1.4 Hz, 1H, H-3), 7.06 (d, J = 1.5 Hz, 1H, H-3′), 6.98 (d, J = 1.4 Hz, 1H, H-5′), 2.89 (dd, J = 12.5, 5.9 Hz, 1H, H-α), 2.70 (dd, J = 12.5, 7.5 Hz, 1H, H-α′), 1.66 (m, 1H, H-β), 1.53 (m, 1H, H-γ), 1.25 (m, 1H, H-γ′), 1.02 (d, J = 6.6 Hz, 3H, γ-CH_3), 0.89 (t, J = 7.4 Hz, 3H, δ-CH_3). ^{13}C NMR (100.61 MHz, $CDCl_3$, TMS δ): 138.6 (C-2), 135.8 (C-2′), 133.8 (C-4′), 130.9 (C-3), 127.6 (C-5), 126.4 (C-3′), 121.6 (C-5′), 77.6 (C-4), 42.5 (C-α), 34.6 (C-β), 28.5 (C-γ), 18.9 (C-γ′), 11.1 (C-δ). Elemental analysis $C_{13}H_{15}IS_3$ Calcd: C, 39.59; H, 3.83; S, 24.39. Found: C, 39.48; H, 3.87; S, 24.22.

General Procedure for the Oxidative Coupling with $FeCl_3$. Bithiophenes **1**−**5** were dissolved in chloroform, then a suspension of $FeCl_3$ (4:1 molar ratio) in nitromethane was slowly added (1 h). The mixture was stirred at room temperature for 20 h, and after evaporation of the solvent, the residue was stirred (1 h) with a solution of methanol and HCl 1 N. After removal of the solvent, the dark product formed was Soxhlet-extracted with methanol (24 h), *n*-pentane (24 h), and chloroform (24 h). The octamers were recovered from the chloroform phases.

Synthesis of OT1. Bithiophene **1** (0.20 g, 0.6 mmol) in chloroform (10 mL) and $FeCl_3$ (0.38 g, 2.4 mmol) in nitromethane (10 mL) gave 0.15 g (75%) of octithiophene. HPLC: 90%. MIC−IR (neat): 3104 (w), 3072 (w), 3062 (w), 2955 (m), 2922 (m), 2869 (w), 2851 (m), 1487 (m), 1468 (m), 1455 (m), 1417 (w), 1377 (w), 1278 (w), 1220 (w), 925 (w), 852 (w), 825 (m), 809 (m), 784 (m), 721 (m). MS (EI) *m*/*z*: 1234 (100, $M^{+\bullet}$), 146 (39, $C_8H_{18}S$), 36 (62, C_6H_{11}), 70 (50, C_5H_{10}), 56 (54, C_4H_8). Elemental analysis $C_{64}H_{82}S_{12}$ Calcd: C, 62.19; H, 6.69; S, 31.13. Found: C, 62.26; H, 6.72; S, 30.95.

Synthesis of OT2. Bithiophene **2** (0.40 g, 1 mmol) in chloroform (17 mL) and $FeCl_3$ (0.66 g, 4 mmol) in nitromethane (17 mL) gave 0.36 g (55%) of octithiophene. HPLC: 60%. MIC−IR (neat): 3111 (w), 3072 (w), 3055 (w), 2954 (m), 2924 (m), 2868 (w), 2851 (m), 1476 (m), 1467 (sh), 1441 (sh), 1377 (w), 1262 (w), 930 (w), 869 (w), 819 (m), 796 (sh), 720 (w). MS (EI) *m*/*z*: 1552 (<1, M + $6^{+\bullet}$), 146 (55, $C_8H_{18}S$), 80/82 (62, HBr), 69 (71, C_5H_9), 55 (100,

Scheme 2

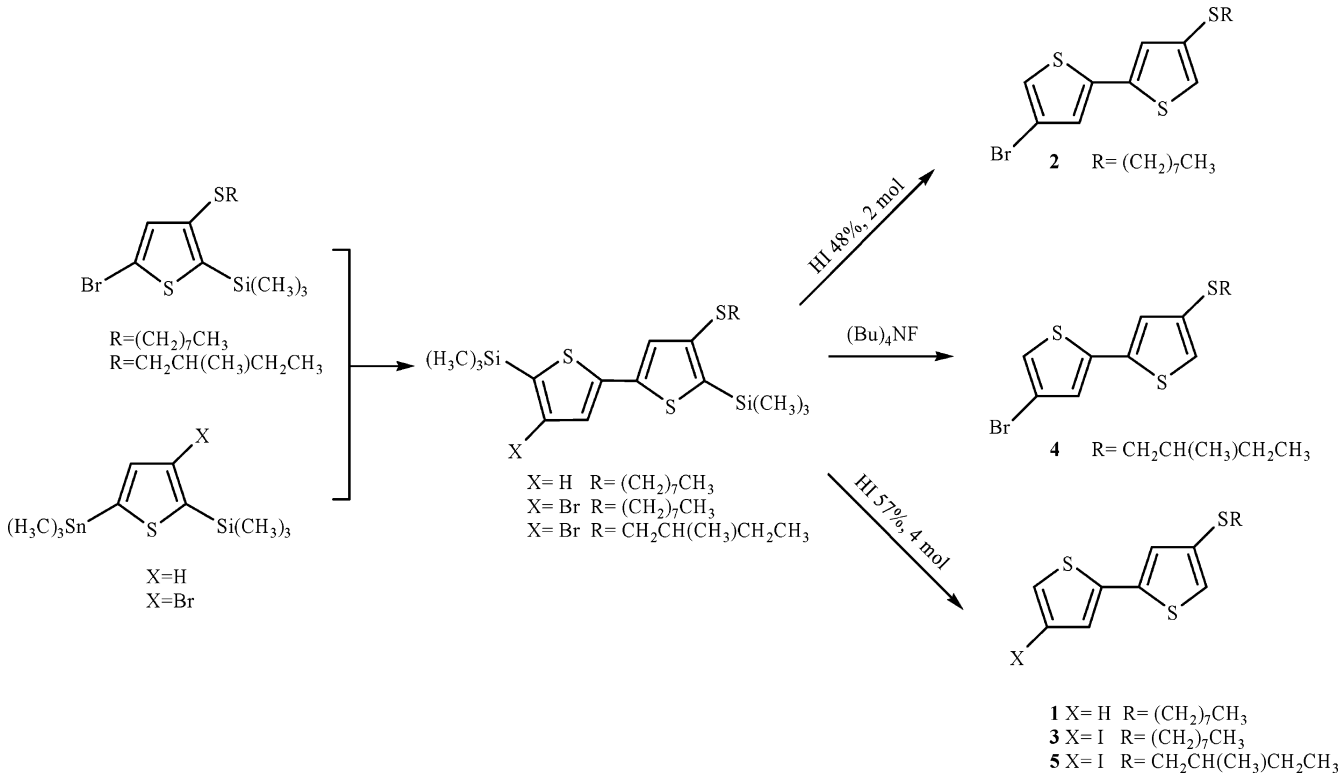

C_4H_7). Elemental analysis $C_{64}H_{78}Br_4S_{12}$ Calcd: C, 49.54; H, 5.07; S, 24.80. Found: C, 49.63; H, 5.03; S, 24.55.

Synthesis of OT3. Bithiophene **3** (1.20 g, 3 mmol) in chloroform (50 mL) and $FeCl_3$ (1.9 g, 12 mmol) in nitromethane (50 mL). Yield: 0.97 g, 83%. HPLC: 75%. MIC−IR (neat): 3103 (w), 3076 (sh), 2954 (m), 2931 (m), 2856 (m), 1477 (m), 1466 (m), 1459 (sh), 1376 (w), 927 (w), 865 (w), 820 (m), 793 (w), 728 (w). MS (EI) *m*/*z*: 1486 (<1, $M^{+\bullet}$ − 2I + 2H), 254 (20, I_2), 146 (56, $C_8H_{18}S$), 128 (81, HI), 71 (87, C_5H_{11}), 57 (100, C_4H_9). Elemental analysis $C_{64}H_{78}I_4S_{12}$ Calcd: C, 44.18; H, 4.52; S, 22.12. Found: C, 44.15; H, 4.57; S, 21.88.

Synthesis of OT4. Bithiophene **4** (0.20 g, 0.6 mmol) in chloroform (10 mL) and $FeCl_3$ (0.38 g, 2.4 mmol) in nitromethane (10 mL) gave 0.10 g (53%) of octithiophene. HPLC: 85%. MIC−IR (neat): 3107 (w), 3080 (w), 3059 (w), 2961 (m), 2925 (m), 2871 (m), 2854 (m), 1546 (w), 1480 (m), 1460 (m), 1378 (m), 929 (m), 872 (m), 840 (m), 821 (m), 811 (sh), 730 (w). MS (EI) *m*/*z*: 1384 (<1, M + $6^{+\bullet}$), 104 (8, $C_5H_{11}S$), 79/81 (40, Br), 70 (47, C_5H_{10}), 55 (100, C_4H_7). Elemental analysis $C_{52}H_{54}Br_4S_{12}$ Calcd: C, 45.15; H, 3.93; S, 27.81. Found: C, 45.11; H, 3.98; S, 27.67.

Synthesis of OT5. Bithiophene **5** (0.30 g, 0.8 mmol) in chloroform (13 mL) and $FeCl_3$ (0.5 g, 3.2 mmol) in nitromethane (13 mL) gave 0.23 g (70%) of octithiophene. HPLC: 85%. MIC−IR (neat): 3098 (w), 3078 (w), 3058 (w), 2964 (m), 2928 (m), 2871 (m), 2857 (m), 1478 (m), 1459 (m), 1378 (m), 930 (m), 867 (m), 838 (sh), 825 (m), 793 (m), 736 (w). MS (EI) *m*/*z*: 1570 (<1, $M^{+\bullet}$), 254 (85, I_2), 127 (58, I), 104 (39, $C_5H_{12}S$), 70 (100, C_5H_{10}), 55 (98, C_4H_7). Elemental analysis $C_{52}H_{54}I_4S_{12}$ Calcd: C, 39.75; H, 3.46; S, 24.49. Found: C, 39.81; H, 3.49; S, 24.15.

Computational Methods. All calculations were performed with the Gaussian03[23] program package. Becke's three-parameter functional with nonlocal correlation provided by the Perdew/Wang expression (B3PW91)[24] combined with the economical but well balanced MIDI![25] basis set was used. The hybrid spin unrestricted DFT wave functions were employed for open shell systems. Geometry optimizations were carried out on all reactants, products, and transition states, and then harmonic frequency confirmed the identity of stationary states.

The molecular electrostatic potential maps (MEP)[26] of the optimized geometry structures of oligothiophenes were calculated at the same level of theory and plotted using Gaussview.[27] Molecular electrostatic potential maps are reported onto 0.0004 e/bohr^3 isosurface of electrodensity, and representations of SOMO orbital isodensity refer to an isovalue of 0.025.

Results

Synthesis. α,α′-Bithiophenes are the most simple oligomers and can be used as starting materials for the synthesis of longer macromolecules. The Stille-type coupling between a tin and a haloderivative was the procedure followed to generate bithiophenes[13] **1**−**5** (Scheme 2).

Bithiophenes **1**-**5** were prepared from 4-X-4′-(alkylsulfanyl)-5,5′-bis(trimethylsilyl)-2,2′-bithiophenes (X = Br, H) through desilylation. When HI 58% was used as the desilylating agent, the bromine derivatives were simultaneously desilylated and iodinated. 4-X-4′-(alkylsulfanyl)-5,5′-bis(trimethylsilyl)-2,2′-bithiophenes (X = Br, H) were in turn obtained by coupling 3-(alkylsulfanyl)-5-bromo-2-(trimethylsilyl)thiophene and 2-(trimethylsilyl)-5-(trimethylstannyl)thiophene or 3-bromo-2-(trimethylsilyl)-5-(trimethylstannyl)thiophene in the presence of a palladium(0) catalyst.

Octithiophenes **OT1**−**OT5** were synthesized from the corresponding bithiophenes **1**−**5** by oxidative polymerization with $FeCl_3$ in $CH_3NO_2/CHCl_3$ (Scheme 1) in 50−80% yield of separated product. Octithiophenes **OT2** and **OT4** give red-green free-standing films easily detachable from the glassware, while **OT1**, **OT3** and **OT5** are red-orange scaly solids.

NMR and MS Characterization. The regiochemistry of octithiophenes **OT1**−**OT5** and the complete assignment of ^{1}H and ^{13}C resonances were determined through NMR ^{1}H,^{13}C inverse-detection techniques, which have already been successfully used in the interpretation of the regiochemistry of OTs and PTs.[28]

The ^{1}H NMR spectrum of **OT1** reported in Figure 1, as an example, displays a pair of doublets at 7.30 and 7.15 ppm, characterized by a β,β′-coupling constant J = 3.8 Hz, three

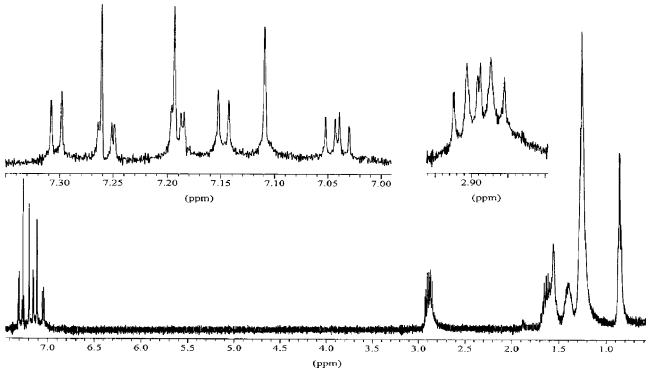

Figure 1. ^{1}H NMR spectrum of octithiophene **OT1**.

Chart 1

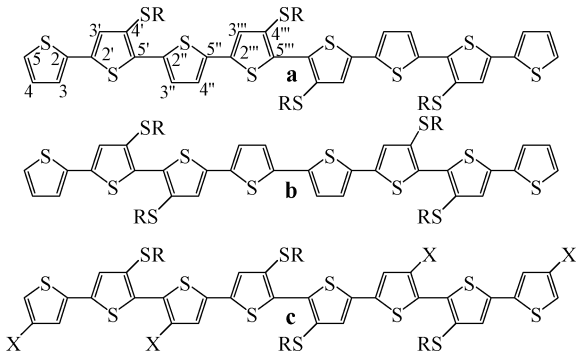

double doublets of an AMX system at 7.26, 7.19 and 7.04 ppm, characterized by three coupling constants J = 1.0, 5.2, and 3.7 Hz, respectively, two singlets at 7.11 and 7.19 ppm, two overlapped triplets at 2.91 (2H) and 2.88 ppm (2H), a multiplet at 1.65 ppm (4H), two broad signals at 1.41 (4H) and 1.28 ppm (16H), and a triplet at 0.88 ppm (6H).

The coupling pattern of the aromatic protons indicates that a 2,5-disubstituted, two trisubstituted, and one 2-monosubstituted thiophene rings are present, and the two triplets around 2.9 ppm point to the presence of two different octylsulfanyl chains. ^{1}H NMR spectrum of **OT1** is compatible with two possible structures, **a** and **b**, corresponding to symmetric octithiophenes (Chart 1).

The HMQC[29] spectrum of the aromatic region allows us to identify all directly bonded H,C pairs to confirm that all protons, except H-5 at 7.26 ppm, are β-protons (^1J(H,C) $\approx$ 170 Hz) and to rule out the formation of α,β-coupling between thiophene units.

The identification of the quaternary carbons coupled to protons through intraring long-range coupling constants around 10 Hz or less was made by running two HMBC[30] experiments with evolution delays of 50 and 100 ms.

The analysis of the complex correlation pattern permits the unambiguous assignment of all proton and carbon signals, as reported in Tables 1 and 2, and the reconstruction of an octithiophene skeleton which corresponds to structure **a** in Chart 1. For this assignment is particularly diagnostic the presence of an interring correlation between proton H-3″ and carbon C-5′.

The ^{1}H NMR spectra of **OT2**−**OT5** display, in the aromatic region, a pair of doublets characterized by a coupling constant J = 1.4 Hz, and three singlets indicating the presence of a 2,4-disubstituted and of three trisubstituted rings in the oligomeric backbone. Signals from two different alkyl chains are found in the aliphatic region.

The HMQC and HMBC experiments enable the contextual detection and assignment of aromatic carbon signals of each thiophene ring to be made, and they permit establishing that the first ring bears a halogen in the 4-position and to assign the alkylsulfanyl chain bonded to C-4′. Unfortunately, the correlation between H-3′ and C-2″ (or between H-4″ and C-5′) was not detected, and we could not establish if the third ring bears a halogen or an alkylsulfanyl group in 3″ position. The problem was overcome through a halogen−hydrogen exchange by treatment of **OT2**−**OT5** with butyllithium. The ^{1}H NMR spectra of the octithiophenes thus dehalogenated correspond to that of **OT1**, indicating that their regiochemistry is that depicted by structure **c** in Chart 1, i.e., the third thiophene ring is that bearing the halogen atom.

Mass spectra, acquired under electron impact conditions after direct insertion of solid samples and heat induced vaporization, confirm that our oligomers are octithiophenes as deduced by NMR measurements. All mass spectra show the peak of the molecular ion along with the correct isotopic cluster; only for **OT3**, the peak at higher m/z values corresponds to a partially deiodinated species.

UV−Vis and CD Spectroscopy. UV−Vis spectroscopy is a highly responsive technique for the investigation of conformational changes and intermolecular interactions of conjugated systems in solution and in the solid state. Solutions of octithiophenes **OT1**−**OT5** in chloroform (good solvent) show a broad and unstructured absorption band with λ_{max} values (Table 3) very similar to that reported for a HT regioregular octadecyl octithiophene-5-carboxylic acid benzyl ester (λ_{max} 427 nm),[31] 50−20 nm blue-shifted with respect to regioregular HH-TT poly(alkylsulfanyl)thiophenes[14,15] and 80−50 nm blue-shifted with respect to a regioregular HT poly(butylsulfanyl)thiophene.[32]

These absorptions are attributable to the $\pi-\pi^*$ transitions and reflect the conformational freedom of the thienyl backbones. It is observed that the λ_{max} of iodinated octithiophenes **OT3** and **OT5** is lower than that of the brominated ones **OT2** and **OT4**, which in turn is lower than that of nonhalogenated **OT1**. This trend parallels that of the higher steric hindrance of the iodine and bromine atoms with respect to hydrogen that induce

Table 1. ^{1}H NMR Data (δ, ppm) for Octithiophenes OT1−OT5

compound	H-3	H-4	H-5	H-3′	H-3″	H-4″	H-3‴	chain	C$H_2(\alpha)$	C$H_2(\beta)$	C$H_2(\gamma)$	C$H_2(\delta)$	C$H_2(\epsilon)$	C$H_2(\zeta)$	C$H_2(\eta)$	C$H_3(\theta)$
OT1	7.19	7.04	7.26	7.11	7.30	7.15	7.19	4′−	2.91	1.65	1.41	1.28	1.28	1.28	1.28	0.88
								4‴−	2.88	1.65	1.41	1.28	1.28	1.28	1.28	0.88
OT2	7.13		7.17	7.16		7.17	7.19	4′−	2.85	1.60	1.37	1.25	1.25	1.25	1.25	0.87
								4‴−	2.86	1.60	1.37	1.25	1.25	1.25	1.25	0.87
OT3	7.19		7.33	7.16		7.25	7.18	4′−	2.83	1.59	1.38	1.25	1.25	1.25	1.25	0.86
								4‴−	2.86	1.61	1.36	1.25	1.25	1.25	1.25	0.86
								chain	C$H_2(\alpha)$	C$H(\beta)$	C$H_2(\gamma)$	C$H_3(\gamma')$	C$H_3(\delta)$			
OT4	7.13		7.17	7.16		7.17	7.19	4′−	2.88/2.70	1.62	1.50/1.24	1.00	0.89			
								4‴−	2.90/2.72	1.62	1.50/1.24	1.01	0.89_5			
OT5	7.19		7.33	7.16		7.25	7.17	4′−	2.87/2.68	1.62	1.50/1.25	0.97	0.88			
								4‴−	2.89/2.71	1.62	1.50/1.25	1.00	0.89			

Table 2. ^{13}C NMR Data (δ, ppm) for Octithiophenes OT1−OT5[a]

compound	C-2	C-3	C-4	C-5	C-2′	C-3′	C-4′	C-5′	C-2″	C-3″	C-4″	C-5″	C-2‴	C-3‴	C-4‴	C-5‴
OT1	136.4	124.1	128.0	125.0	134.6	128.3	128.8	134.4	134.9	126.7	123.9	136.8	136.9	127.1	132.6	131.6
OT2	137.3	126.6	110.6	122.1	136.0	127.6	133.8	130.5	128.7	112.1	127.0	137.4	135.2	127.8	132.8	132.3
OT3	138.1	131.4	77.8	128.2	136.3	127.4	134.3	131.6	133.0	84.3	132.2	139.6	135.1	127.9	132.8	132.4
OT4	137.2	126.5	110.4	122.1	135.8	127.5	133.9	130.0	128.4	112.0	127.0	137.7	135.0	127.7	132.8	132.0
OT5	138.0	131.4	77.8	128.1	136.1	127.4	134.7	131.2	132.8	84.4	132.2	139.8	134.8	127.8	132.9	132.2

	chain	$CH_2(\alpha)$	$CH_2(\beta)$	$CH_2(\gamma)$	$CH_2(\delta)$	$CH_2(\epsilon)$	$CH_2(\zeta)$	$CH_2(\eta)$	$CH_3(\theta)$
OT1	4′−	36.37	29.65	28.75	29.2	29.2	31.75	22.63	14.15
	4‴−	36.33	29.65	28.75	29.2	29.2	31.75	22.63	14.15
OT2	4′−	36.17	29.48	28.68	29.2	29.2	31.80	22.65	14.11
	4‴−	36.44	29.48	28.74	29.2	29.2	31.80	22.65	14.11
OT3	4′−	35.95	29.50*	28.67#	29.18§	29.11§	31.81	22.66	14.11
	4‴−	36.44	29.55*	28.75#	29.21§	29.14§	31.81	22.66	14.11

	chain	$CH_2(\alpha)$	$CH(\beta)$	$CH_2(\gamma)$	$CH_3(\gamma')$	$CH_3(\delta)$
OT4	4′−	43.6	34.7	28.4	18.6	10.8
	4‴−	43.3	34.7	28.4	18.6	10.8
OT5	4′−	43.0	34.9	28.6	18.8	11.2
	4‴−	43.6	34.9	28.7	18.8	11.2

[a] The directly acquired ^{13}C NMR spectra display only aliphatic signals; the aromatic carbon chemical shifts derive from inverse-detection experiments (lower resolution). *, #, § Denote interchangeable assignments.

Table 3. Relevant UV Data for Octithiophenes OT1−OT5 and Related Poly(alkylsulfanyl)Thiophenes

compound	λ_{max} ($CHCl_3$, nm)	ϵ (mol^{-1} L cm^{-1})	λ_{max} ($CHCl_3/CH_3OH$, nm)
OT1	456	1.1×10^7	
OT2	435	6.2×10^7	468, 500, 540, 584
OT3	419	4.2×10^7	
OT4	430	5.0×10^7	458, 502, 542, 590
OT5	419	3.5×10^7	
a	502		515, 555, 600
b	470−466		520, 560, 610
c	469		530, 565, 623

[a] Regioregular HT poly(butylsulfanyl)thiophene.[32] [b] Regioregular HH−TT poly(alkylsulfanyl)thiophenes.[14] [c] Chiral regioregular HH−TT poly-(alkylsulfanyl)thiophene.[15]

a distortion in the planarity of the backbone, which translates into a decrease in effective conjugation length and into a blue-shift of the optical absorption.

To gain a deeper insight into the conformational and aggregation properties of OTs, UV−Vis spectra were recorded in $CHCl_3/CH_3OH$ mixtures (Figure 2).

A marked difference in the solvatochromic behavior of the brominated **OT2** and **OT4** (spectrum not shown, but similar to that of **OT2**) with respect to the nonhalogenated **OT1**, and the iodinated **OT3** and **OT5** (spectrum not shown, but very similar to that of **OT3**) is found. A significant red-shift, accompanied by the formation of a fine vibronic structure in the absorption curves, occurs in the case of **OT2** and **OT4** by increasing the methanol-to-chloroform ratio, or in thin films, whereas **OT1**, **OT3** and **OT5** show a lower solvatochromism. In the case of **OT1** and **OT4** spectra are also affected by the formation of a precipitate at high methanol percentages.

The red-shift and the appearance of the vibronic structure after addition of a nonsolvent is typical of regioregular HT polyalkylthiophenes[33,34] and of regioregular (HT and HH-TT) poly(alkylsulfanyl)thiophenes,[14,15,32] and it is often attributed to a planarization of the backbone and then to an aggregation process, which give rise to the new vibronic bands. This behavior has been observed only in few cases when OTs are concerned,[35] whereas a blue-shift has been reported for some sexithiophenes.[36] The positions of the vibronic bands of **OT2** and **OT4** are very similar to those reported for a thermochromic undecathiophene α,ω-disubstituted with dendritic wedges[37] and are only 20−30 nm blue-shifted with respect to those observed for poly(alkylsulfanyl)thiophenes.[14,15,32] Evidently, the bromine atoms permit a more planar conformation to be achieved by the octithiophenes **OT2** and **OT4** in the presence of high amounts of nonsolvent, while the small hydrogen and the bulky iodine atoms do not. We suppose that the peculiar difference between the absorption properties of our OTs in the absence and in the presence of a poor solvent derives from a compromise between steric interactions and packing forces, related to the different polarizability of hydrogen, bromine, and iodine atoms. Probably only in the case of bromine, the packing forces are strong enough to overcome the steric distortions and induce planarity through stacking interactions.

Circular dichroism (CD) measurements made on films of **OT4**, slowly cast from chloroform or THF, and on chloroform solutions of **OT4** in the presence of a high percentage of methanol, show the presence of a bisignate Cotton effect (Figure 3), as has been previously observed for polythiophenes[34,38,39] and OTs carrying chiral side chains.[36,40] Interestingly, **OT5** does not develop any CD signal neither in solution nor in the solid state.

CD has been observed on chiral OTs and polythiophenes in the presence of aggregates,[15,34,36,38,39,41,42] and only a few cases of CD at the single molecule level are reported for chiral polythiophenes.[39] An interchain mechanism, based on the formation of chiral superstructures,[42] is almost certainly involved in optical activity of OTs, nevertheless the development of CD induced by aggregation only in OTs longer than five−six thiophenic units[36,40] does not permit excluding an interplay between intrachain and interchain factors.

DFT Calculations on the Oligomer Growth. The computational study was carried out at the B3PW91/MIDI! level on 4-(methylsulfanyl)-2,2′-bithiophene, with the aim to establish the possible sequence of the coupling reactions, leading to the formation of the octithiophene with the experimental regiochemistry. Unsymmetrical substrates can react, leading to the formation of regioisomers, which differ by the relative position of the substituents. The experimental regiochemistry of the final octithiophene, one inner HH and two lateral HT junctions, which depends on the mode of coupling of the monomers, give relevant information on the mechanism of the oligomerization.

The theoretical approach was focused on the calculation of the Gibbs free energy of activation of competitive coupling

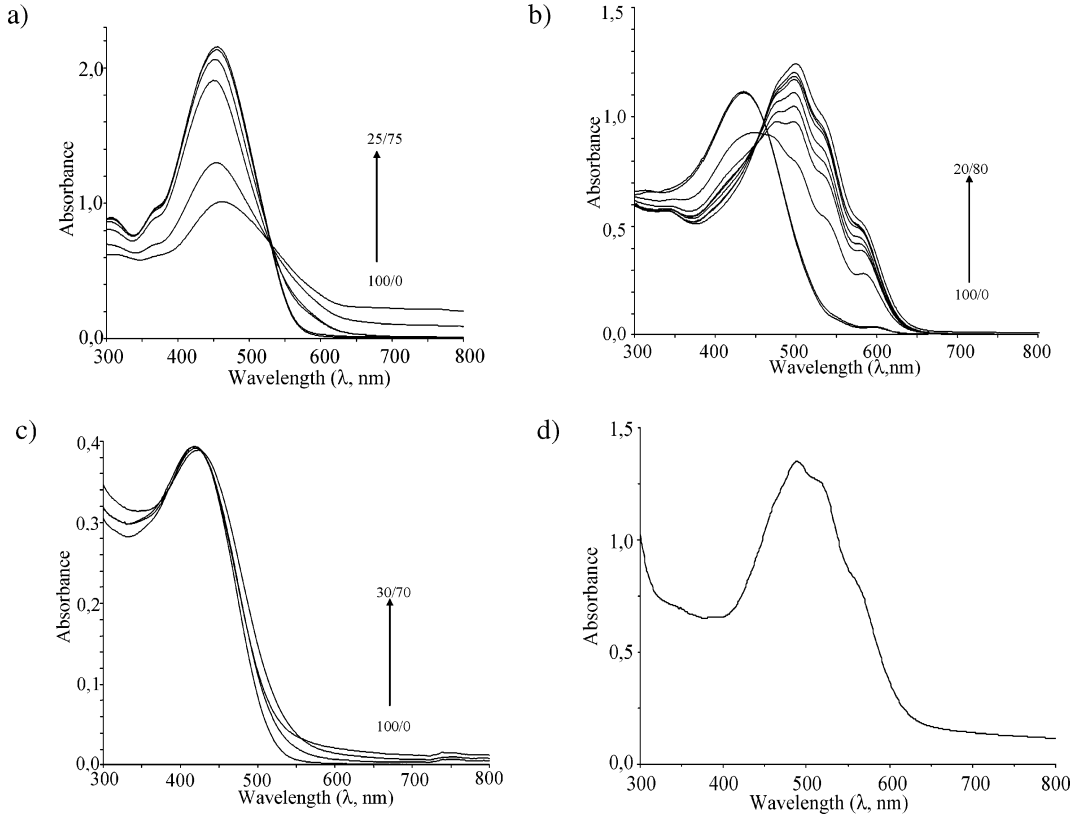

Figure 2. UV−Vis spectra in $CHCl_3/CH_3OH$ mixtures of (a) **OT1**, (b) **OT2**, (c) **OT3**, and (d) **OT2** in thin film.

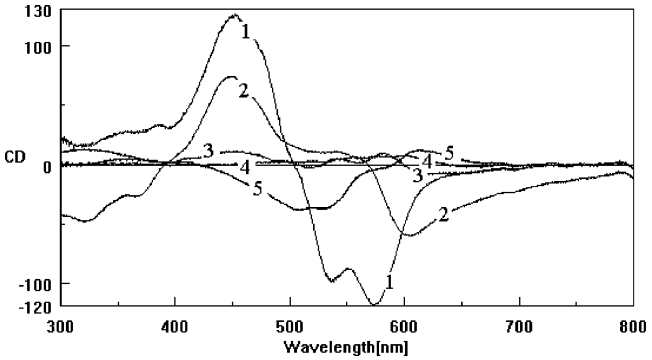

Figure 3. CD spectra of **OT4** films, cast under slow evaporation conditions (1) from THF, (2) from chloroform, and cast under fast evaporation conditions (3) from chloroform, (4) from THF. **(**5) CD solution spectrum in chloroform/methanol 1:9 mixture.

reactions to compare the relative probabilities of the different reaction pathways, as has been already carried out in the case of oligopyrroles and oligothiophenes.[43] It has been shown[44,45] that the calculated unpaired-electron spin-density distribution, orbital analysis, and charge distribution in the radical cations involved in the oxidative coupling provide important information that can be used to predict the reaction sites of the polymerization process. Thus, molecular electrostatic potential maps[26] and semioccupied molecular orbitals (SOMO) were calculated for selected oligomers in order to rationalize the evolution of the electronic structure with the chain growth. This approach offers an insight into the effect of the substituents on the reactive sites (Cα) and an indication of the driving forces for bond formation.

Two mechanisms have been proposed for the oxidative coupling of heteroaromatic rings, i.e., the coupling between two radical cations (RC−RC) or the attack of one radical cation on the neutral substrate. Our approach, which compares the transition state energies corresponding to different RC−RC coupling reaction pathways, is based on recent conclusions reported for five-ring heterocyclic oligomers,[46,47] which have demonstrated that these reactions involve the coupling between two radical cations, and that the subsequent deprotonation processes are fast.[47]

Scheme 3 displays a representation of the RC−RC mechanism applied to a selected reaction pathway, the HT one, and the following considerations are valid for all the reaction pathways considered in our analysis (i.e., also the HH and the TT ones). To simplify the discussion, we labeled the two rings of the starting monomer as **A** for the ring without substituent (tail) and **B** for the ring with substituent (head). The most stable conformation calculated for the radical cation of the starting monomer **AB** ($\mathbf{AB}^{+\bullet}$) is the fully coplanar one, with the two rings trans to each other and the methylsulfanyl groups in the same plane of the thiophene rings. The structure of the HT transition state is characterized by the two monomers parallel but not on the same plane and by the distortion of the Cα hydrogens from the planar geometry. This orientation facilitates the overlap between the two $2p_z$ orbitals of the interacting Cα, that is the initial stage of the σ-type orbital formation. The distance between the two reactive carbons becomes shorter, and their hybridization moves to sp^3 during the formation of the dimeric dication intermediate. The final step is represented by the loss of the two protons, which restores the aromaticity of the two rings.

The various reaction pathways, which could be involved in the formation of octithiophenes, are shown in Scheme 4, together with the calculated free energy barriers $\Delta G^{\dagger}$ for each transition state. The number of the coupling steps leading to octithiophenes can be two or three, depending on the substrates involved in the second step. For each step, we compare the activation energy of all the possible regioisomeric attacks, but only the substrates

Scheme 3. Multistep RC−RC Mechanism for the HT Coupling

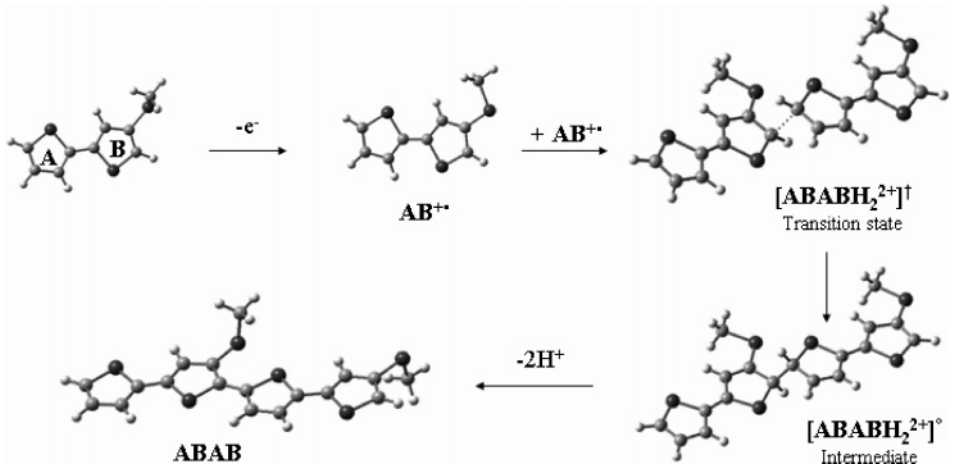

Scheme 4. Free Activation Energies $\Delta G^{\dagger}$ (Numbers over the Arrows, in kcal/mol) Calculated for Selected Coupling Reactions Involving the Monomer AB in Various Reaction Pathways and Leading to Octithiophenes (See the Text for Further Details)[a]

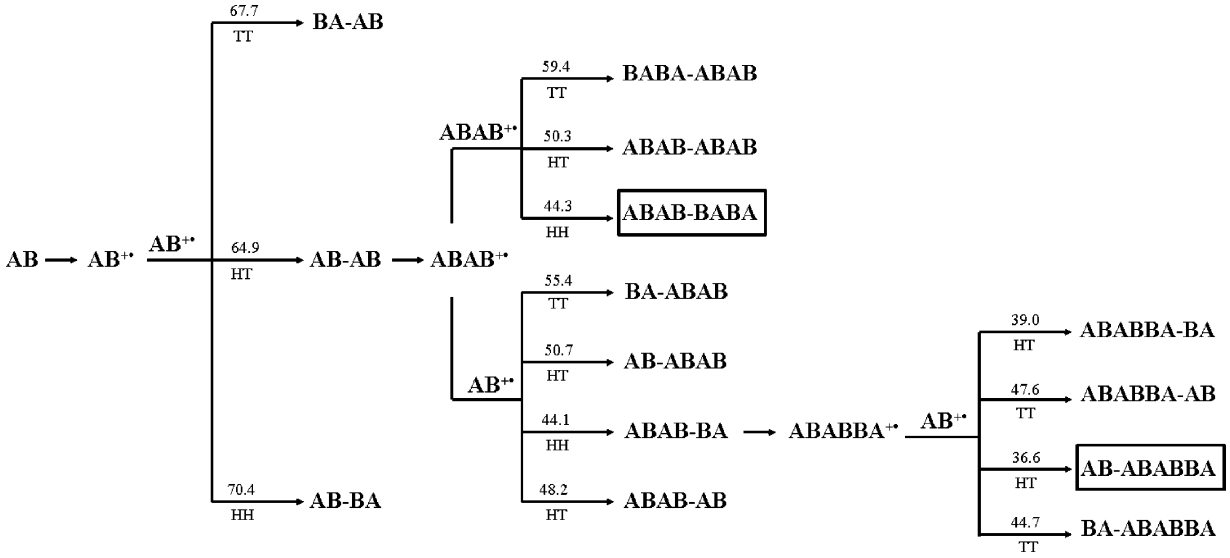

[a] The two octithiophenes deriving from the two competitive routes are squared.

deriving from the transition states with the lower activation barrier are considered as reactive in the successive step.

Three isomeric quaterthiophenes characterized by different inner junctions, **AB−AB**, **AB−BA**, and **BA−AB**, can be formed in the first step. The free activation energy for the HT coupling (**AB−AB**) is 6 and 3 kcal/mol lower than those calculated for the HH and TT couplings, respectively. Hence, the quaterthiophene **ABAB** is that most probably formed in the first step. Its radical cation (**ABAB**$^{+\bullet}$) can react with another **ABAB**$^{+\bullet}$ unit or with a **AB**$^{+\bullet}$ unit in the second step. For each of these reactions, all isomeric couplings were considered.

In the first case, the dimerization process leads directly to the formation of octithiophenes. The free activation energy for the HH coupling (**ABAB−BABA**) is 6 and 15 kcal/mol lower than those calculated for the HT and TT couplings, respectively. A similar result is obtained in the second case, which can be viewed as a chain growth process: three hexamers can form (two out of four pathways lead to the equivalent **ABAB−AB** and **AB−ABAB** sexithiophenes) and the free activation energy for the HH coupling (**ABAB−BA**) is 4, 6, and 10 kcal/mol lower than those calculated for the two HT and TT couplings, respectively. A further step is necessary to obtain an octithiophene, i.e., the coupling of the radical cation of the asymmetric hexamer, **ABABBA** (**ABABBA**$^{+\bullet}$) with one **AB**$^{+\bullet}$ unit. Four different isomers can be generated, and in this case, the calculated activation energies for the two HT couplings are 5−10 kcal/mol lower than those for the TT ones. The $\Delta G^{\dagger}$ of the two HT couplings differ by 3 kcal/mol, and the route with the lower activation energy (generating the **ABABABBA** octithiophene) does not lead to the isomer experimentally observed (**ABABBABA**), which is obtained through the other HT coupling.

Our approach, based on transition state calculations of successive coupling reactions, predicts that the HT is the favorite coupling in the first step, whereas the HH is favorite in the second one. In the third possible step (i.e., coupling between a sexithiophene and a bithiophene), the HT attacks are favorite compared to the TT ones. Regarding the dimerization (two steps) and the chain-propagation (three steps) mechanism, we found that they seem to have nearly the same energy barriers at the second step, suggesting a possible competition between them. Nevertheless, the last route leads to the formation of an octithiophene with a regiochemistry that is not that experimentally observed, and this supports the dimerization process.

The change predicted for the regioselectivity of the coupling steps (i.e., HT for the first and HH for the second one) could be explained as a consequence of the evolution of two electronic effects with the oligomer length. These effects are related to

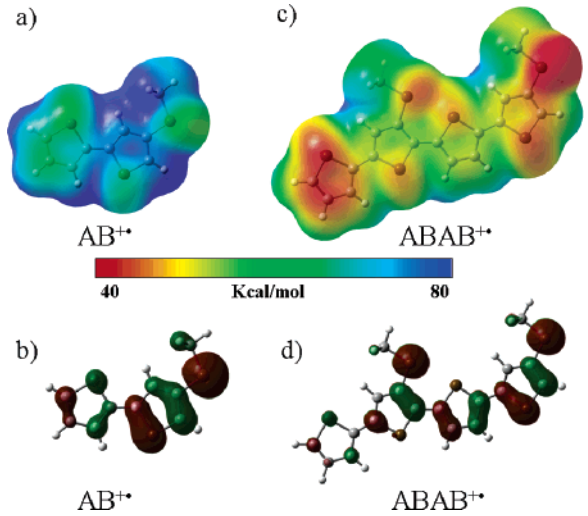

Figure 4. Molecular electrostatic potential maps (a and c) and SOMO (b and d) isosurfaces for **AB**$^{+\bullet}$ and **ABAB**$^{+\bullet}$.

the SOMO density and to the charge distribution in the reacting radical cations and act on the value of the energy barrier, as has already been discussed by Lacroix et al. for the study of polypyrrole growth.[44] Figure 4 shows the SOMO orbital and the molecular electrostatic potential maps for **AB**$^{+\bullet}$ and **ABAB**$^{+\bullet}$, which provide an insight into the results obtained. Concerning **AB**$^{+\bullet}$, a higher (blue) and a lower (green) positive electrostatic potential for the **B** and the **A** ring, respectively, are shown in the molecular electrostatic potential plot (Figure 4a), whereas SOMO, delineating the areas where the unpaired electron is most localized, involves more the π system of the **B** ring than that of **A** (Figure 4b). The charge and the unpaired electron distributions, related to the electrostatic potential (Figure 4c) and to the SOMO (Figure 4d), respectively, become appreciably diffused on the whole substrate in the case of **ABAB**$^{+\bullet}$. It is to be noted that the electrostatic potential values, as well as the shape of the SOMO, on the terminal Cα of the outer **B** ring are significantly smaller if compared with those of the corresponding to the Cα in **AB**$^{+\bullet}$.

On the basis of the above considerations, in the first coupling step (between two **AB**$^{+\bullet}$ units), the HH coupling is favored by the frontier orbital interaction, but the strong electrostatic repulsion between the outer Cα of the **B** rings turns out to be directing the reaction toward the HT coupling. The decreasing of the electrostatic potential of **ABAB**$^{+\bullet}$, and in particular close to the Cα of the outer **B** ring, with respect to **AB**$^{+\bullet}$, reduces the repulsion between the two reactive centers in the second coupling step. Therefore, the frontier orbital interaction, which still favors the HH coupling, has a greater influence than the electrostatic repulsion on the energy barrier.

The last point concerns the reason the reaction does not proceed effectively toward the formation of a polymer. In our opinion, this behavior should be explained by considering the reduced reactivity of the external Cα due to the low localization of SOMO on these atoms in the radical cation of the octithiophene **ABABBABA**, as depicted in Figure 5. A similar behavior, observed also for the oxidative coupling of 3,3′-bis(butylsulfanyl)-2,2′-bithiophene and of 3-(butylsulfanyl)-2,2′-bithiophene (which form hexamers)[16,17] but not for that of 4,4′-bis(alkylsulfanyl)-2,2′-bithiophenes (which readily polymerize),[14,15] suggests that the low SOMO localization at the outer Cα is directly linked to the lack of alkylsulfanyl groups close to them in the intermediate oligomeric radical cations. Further work aimed at deriving a theoretical rationalization of the whole of these experimental results is needed.

Conclusions

In this paper, we present the study of the oxidative polymerization with $FeCl_3$ of 4-(octylsulfanyl)-2,2′-bithiophene and of four TT bithiophenes bearing alkylsulfanyl chains and halogens as substituents in β-position. Exploiting the ability of the alkylsulfanyl group in driving the regiochemistry of the coupling, we were able to synthesize five octithiophenes with the same regiochemistry. When the substituents are the octylsulfanyl or the 2-methylbutylsulfanyl group and the bromine atom, the octithiophenes possess a pronounced solvatochromism, λ_{max}, close to that observed for long alkylsulfanyl polythiophenes, circular dichroism induced by aggregation (in the case of the chiral substituent), and they appear as free-standing films, that is quite unusual for oligomeric materials. Both the less and the more steric demanding hydrogen and iodine atoms alter the properties of the synthesized molecules, which result in less solvatochromic properties and display lower filmability.

DFT calculations on the model molecule 4-(methylsulfanyl)-2,2′-bithiophene helped us in establishing that the oligomeric growth is the result of a HT coupling step followed by a HH one and in deriving which electronic effect drives the regioselectivity in each step. The orbital and the electrostatic interactions contribute in determining the height of the activation energy barrier, and their relative weights evolve with the elongation of the backbone in the oligomerization process.

The experimental regiochemistry of **OT2**−**OT5**, indicates that the behavior toward oxidative coupling of halogenated alkylsulfanyl bithiophenes **2**−**5** is also clearly dominated by the directing ability of the alkylsulfanyl sulfur atom, and the halogen atom seems to influence the percentage of the **ABABBABA** octithiophene obtained.

The oxidative polymerization is revealed to be a good method for generating symmetric octithiophenes from asymmetric TT alkylsulfanyl bithiophenes, which can be further functionalized, for the bromine and iodine atoms are replaceable by other nucleophiles.

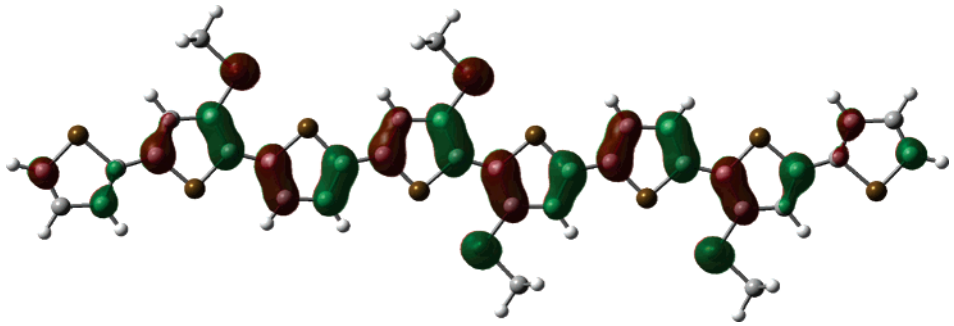

Figure 5. SOMO isosurface for the octithiophene **ABABBABA**$^{+\bullet}$.

Acknowledgment. We thank the Centro Interdipartimentale Grandi Strumenti of the University of Modena and Reggio Emilia for the use of the Bruker DPX-200 and Avance 400 spectrometers, the Perkin-Elmer i-series FT-IR microscope, and the Finnigan MAT SSQ 710 A mass spectrometer, and Prof. A. Forni for the CD measurements.

Supporting Information Available: Coupled HMQC spectrum of **OT1**. Long range $^{1}H,^{13}C$ inverse-detection NMR spectra of **OT1**. This material is available free of charge via the Internet at http://pubs.acs.org

References and Notes

(1) Katz, H. E.; Bao, Z. *J. Phys. Chem. B* **2000**, *104*, 671−678.
(2) Horowitz, G. *Adv. Mater.* **1998**, *10*, 365−377.
(3) Hotta, S.; Waragai, K. *Adv. Mater.* **1993**, *5*, 896−908.
(4) Kovac, J.; Peternai, L.; Lengyel, O. *Thin Solid Films* **2003**, *433*, 22−26.
(5) Furuta, P.; Brooks, J.; Thompson, M. E.; Frechet, J. M. J. *J. Am. Chem. Soc.* **2003**, *125*, 13165−13172.
(6) Huynh, W. U.; Dittmer, J. J.; Janke, J.; Libby, W. C.; Whiting, G. L.; Alivisatos, A. P. *Adv. Funct. Mater.* **2003**, *13*, 73−79.
(7) Liu, J.; Tanaka, T.; Sivula, K.; Alivisatos, A. P.; Frechet, J. M. J. *J. Am. Chem. Soc.* **2004**, *126*, 6550−6551.
(8) Crone, B.; Dodabalapur, A.; Gelperin, A.; Torsi, L.; Katz, H. E.; Lovinger, A. J.; Bao, Z. *Appl. Phys. Lett.* **2001**, *78*, 2229−2231.
(9) Someya, T.; Katz, H. E.; Gelperin, A.; Lovinger, A. J.; Dodabalapur, A. *Appl. Phys. Lett.* **2002**, *81*, 3079−3081.
(10) Kohler, A.; Wilson, J. S.; Friend, R. H. *Adv. Mater.* **2002**, *14*, 701−707.
(11) Destri, S.; Pasini, M.; Botta, C.; Porzio, W.; Bertini, F.; Marchiò, L. *J. Mater. Chem.* **2002**, *12*, 924−933.
(12) Tonzola, C. J.; Maksudul, M. A.; Kaminsky, W.; Jenekhe, S. A. *J. Am. Chem. Soc.* **2003**, *125*, 13548−13558.
(13) Bäuerle, P. In *Handbook of Oligo- and Polythiophenes*; Fichou, D., Ed.; Wiley-VCH: Weinheim, 1999; p 89.
(14) Iarossi, D.; Mucci, A.; Schenetti, L.; Seeber, R.; Goldoni, F.; Affronte, M.; Nava, F. *Macromolecules* **1999**, *32*, 1390−1397.
(15) Iarossi, D.; Mucci, A.; Parenti, F.; Schenetti, L.; Seeber, R.; Zanardi, C.; Forni, A.; Tonelli, M. *Chem.—Eur. J.* **2001**, *7*, 676−685.
(16) Mucci, A.; Parenti, F.; Schenetti, L.; Zanardi, C. *Trends Heterocycl. Chem.* **2001**, *7*, 55−64.
(17) Iarossi, D.; Mucci, A.; Schenetti, L.; Sodini, V. *J. Heterocycl. Chem.* **1999**, *36*, 241−247.
(18) Goldoni, F.; Langeveld-Voss, B. M. W.; Meijer, E. W. *Synth. Commun.* **1998**, *28*, 2237−2244.
(19) Cagnoli, R.; Lanzi, M.; Mucci, A.; Parenti, F.; Schenetti, L. *Synthesis* **2005**, 267−271.
(20) Tour, J. M.; Wu, R. *Macromolecules* **1992**, *25*, 1901−1907.
(21) Frohlich, H.; Kalt, W. *J. Org. Chem.* **1990**, *55*, 2993−2995.
(22) Baumgartner, T.; Bergmans, W.; Kárpáti, T.; Neumann, T.; Nieger, M.; Nyulászi, L. *Chem.—Eur. J.* **2005**, *11*, 4687−4699.
(23) Frisch, M. J.; Trucks, G. W.; Schlegel, H. B.; Scuseria, G. E.; Robb, M. A.; Cheeseman, J. R.; Montgomery, J. A., Jr.; Vreven, T.; Kudin, K. N.; Burant, J. C.; Millam, J. M.; Iyengar, S. S.; Tomasi, J.; Barone, V.; Mennucci, B.; Cossi, M.; Scalmani, G.; Rega, N.; Petersson, G. A.; Nakatsuji, H.; Hada, M.; Ehara, M.; Toyota, K.; Fukuda, R.; Hasegawa, J.; Ishida, M.; Nakajima, T.; Honda, Y.; Kitao, O.; Nakai, H.; Klene, M.; Li, X.; Knox, J. E.; Hratchian, H. P.; Cross, J. B.; Bakken, V.; Adamo, C.; Jaramillo, J.; Gomperts, R.; Stratmann, R. E.; Yazyev, O.; Austin, A. J.; Cammi, R.; Pomelli, C.; Ochterski, J. W.; Ayala, P. Y.; Morokuma, K.; Voth, G. A.; Salvador, P.; Dannenberg, J. J.; Zakrzewski, V. G.; Dapprich, S.; Daniels, A. D.; Strain, M. C.; Farkas, O.; Malick, D. K.; Rabuck, A. D.; Raghavachari, K.; Foresman, J. B.; Ortiz, J. V.; Cui, Q.; Baboul, A. G.; Clifford, S.; Cioslowski, J.; Stefanov, B. B.; Liu, G.; Liashenko, A.; Piskorz, P.; Komaromi, I.; Martin, R. L.; Fox, D. J.; Keith, T.; Al-Laham, M. A.; Peng, C. Y.; Nanayakkara, A.; Challacombe, M.; Gill, P. M. W.; Johnson, B.; Chen, W.; Wong, M. W.; Gonzalez, C.; Pople, J. A. *Gaussian 03*, revision B.04; Gaussian, Inc.: Wallingford, CT, 2004.
(24) Becke, A. D. *J. Chem. Phys.* **1993**, *98*, 5648−5652; Perdew, J. P.; Wang, Y. *Phys. Rev. B* **1992**, *45*, 13244−13248.
(25) Easton, R. E.; Giesen, D. J.; Welch, A.; Cramer, C. J.; Truhlar, D. G. *Theor. Chim. Acta* **1996**, *93*, 281−301.
(26) Murray, J. S., Sen, K. D., Eds. *Molecular Electrostatic Potentials: Concepts and Applications*; Theoretical and Computational Chemistry Book Series, Vol. 3; Elsevier: Amsterdam, 1996.
(27) *GaussView*, version 3.0, Dennington, R., II; Keith, T.; Millam, J.; Eppinnett, K.; Hovell, W. L.; Gilliland, R.; Semichem, Inc.*:* Shawnee Mission, KS, 2003.
(28) Schenetti, L.; Mucci A. In *New Advances in Analytical Chemistry*; Atta-ur-Rahman, Ed.; Taylor & Francis Inc.: New York, 2002; Vol. 3, p 1.
(29) Bax, A.; Griffey, R. H.; Hawkins, B. L. *J. Magn. Reson.* **1983**, *55*, 301−315.
(30) Bax, A.; Summers, M. F. *J. Am. Chem. Soc.* **1986**, *108*, 2093−2094.
(31) Kirschbaum, T.; Azumi, R.; Mena-Osteritz, E.; Bäuerle, P. *New. J. Chem.* **1999**, *23*, 241−250.
(32) Goldoni, F.; Iarossi, D.; Mucci, A.; Schenetti, L.; Zambianchi, M. *J. Mater. Chem.* **1997**, *7*, 593−596.
(33) Kiriy, N.; Jähne, E.; Adler, H.-J.; Schneider, M.; Kiriy, A.; Gorodyska, G.; Minko, S.; Jehnichen, D.; Simon, P.; Fokin, A. A.; Stamm, M. *Nano Lett.* **2003**, *3*, 707−712; Sandstedt, C. A.; Rieke, R. D.; Eckhardt, C. J. *Chem. Mater.* **1995**, *7*, 1057−1059.
(34) Langeveld-Voss, B. M. W.; Janssen, R. A. J.; Meijer, E. W. *J. Mol. Struct.* **2000**, *512*, 285−301.
(35) Kiriy, N.; Kiriy, A.; Bocharova, V.; Stamm, M.; Richter, S.; Plötner, M.; Fischer, W.-J.; Krebs, F. C.; Senkovska, I.; Adler, H.-J. *Chem. Mater.* **2004**, *16*, 4757−4764; Kiriy, N.; Bocharova, V.; Kiriy, A.; Stamm, M.; Krebs, F. C.; Adler, H.-J. *Chem. Mater.* **2004**, *16*, 4765−4771.
(36) Leclère, P.; Surin, M.; Viville, P.; Lazzaroni, R.; Kilbinger, A. F. M.; Henze, O.; Feast, W. J.; Cavallini, M.; Biscarini, F.; Schenning, A. P. H. J.; Meijer, E. W. *Chem. Mater.* **2004**, *16*, 4452−4466 and references herein.
(37) Apperloo, J. J.; Janssen, R. A. J.; Malenfant, P. R. L.; Frechet, J. M. J. *Macromolecules* **2000**, *33*, 7038−7043.
(38) Goto, H.; Yashima, E. *J. Am. Chem. Soc.* **2002**, *124*, 7943−7949; Goto, H.; Okamoto, Y.; Yashima, E. *Macromolecules* **2002**, *35*, 4590−4601; Brustolin, F.; Goldoni, F.; Meijer, E. W.; Sommerdijk, N. A. J. M. *Macromolecules* **2002**, *35*, 1054−1059.
(39) Zhang, Z.-B.; Fujiki, M.; Motonaga, M.; Nakashima, H.; Torimitsu, K.; Tang, H.-Z. *Macromolecules* **2002**, *35*, 941−944; Nilsson, K. P. R.; Johan, J. D. M.; Konradsson, P.; Inganäs, O. *Macromolecules* **2004**, *37*, 6316−6321.
(40) Sakurai, S.; Goto, H.; Yashima, E. *Org. Lett.* **2001**, *3*, 2379−2382.
(41) Langeveld-Voss, B. M. W.; Beljonne, D.; Shuai, Z.; Janssen, R. A. J.; Meskers; S. C. J.; Meijer, E. W.; Bredas, J.-L. *Adv. Mater.* **1998**, *10*, 1343−1348.
(42) Beljonne, D.; Langeveld-Voss, B. M. W.; Shuai, Z.; Janssen, R. A. J.; Meskers, S. C. J.; Meijer, E. W.; Bredas, J.-L. *Synth. Met.* **1999**, 912−913.
(43) Lacroix, J.-C.; Maurel, F.; Lacaze, P.-C. *J. Am. Chem. Soc.* **2001**, *123*, 1989−1996; Lacroix, J.-C.; Maurel, F.; Lacaze, P.-C. *Synth. Met.* **1999**, *101*, 675−676; Yurtsever, M.; Yurtsever, E. *Polymer* **2004**, *45*, 9039−9045.
(44) Lacroix, J.-C.; Valente, R.-J.; Maurel, F.; Lacaze, P.-C. *Chem.—Eur. J.* **1998**, *4*, 1667−1677.
(45) Smith, J. R.; Cox, P. A.; Campbell, S. A.; Ratcliffe, N. M. *J. Chem. Soc., Faraday Trans.* **1995**, *91*, 2331−2338; Ando, S.; Ueda, M. *Synth. Met.* **2002**, *129*, 207−213; Fréchette, M.; Belletête, M.; Bergeron, J.-Y.; Durocher, G.; Leclerc, M. *Synth. Met.* **1997**, *84*, 223−224.
(46) Andrieux, C. P.; Audebert, P.; Hapiot, P.; Savéant, J.-M. *J. Phys. Chem.* **1991**, *95*, 10158−10164; Guyard, L.; Hapiot, P.; Neta, P. *J. Phys. Chem.* **1997**, *101*, 5698−5706; Tschuncky, P.; Heinze, J.; Smie, A.; Engelmann, G.; Kossmehl, G. *J. Electroanal. Chem.* **1997**, *433*, 223−226.
(47) Audebert, P.; Cate, J.-M.; Le Coustumer, G.; Duchenet, V.; Hapiot, P. *J. Phys. Chem.* **1995**, *99*, 11923−11929.

MA0614141